Journal of ELECTRICAL ENGINEERING, VOL 70 (2019), NO3, 218–226

sciendo

PAPERS

Performance optimization of permanent magnet synchronous motor by cogging torque reduction

Vasilija Sarac*

The development of the robotics and the automation and the need for the motors that can work in the applications that require high speed, precision and increased efficiency have led to the increased use of permanent magnet synchronous motors and their continuous development in terms of improving their performance. Cogging torque is one of the features of these types of the motors that deteriorate motor performance especially at low speeds. Therefore, in this paper the method of genetic algorithms (GA) is applied as an optimization tool, for minimizing the cogging torque without changing the other important operating parameters like output power, torque or current. Even more, the optimized motor model has improved efficiency compared to the starting model and has the decreased weight of the permanent magnets. The optimization is done by changing the rotor design in terms of the magnet thickness, pole span and shape of the magnets. Finite elements (FE) models of the optimized and the basic motor were derived and from them the flux density distribution in the motor cross section and in the air gap was calculated. In addition, the improvement of the motor operation is observed from the torque characteristics calculated by the FE models.

K e y w o r d s: cogging torque, synchronous permanent magnet motor, magnetic flux density distribution, genetic algorithms

1 Introduction

Permanent magnet synchronous motor (PMSM) combines the features of the induction motor and the brushless DC motor. Like the brushless DC motor it has a permanent magnet on the rotor instead of the rotor winding, placed in the rotor core (inset permanent magnet motors) or mounted on the rotor surface (surface permanent magnet motors). The stator winding is like the winding of the induction motor, constructed to produce a sinusoidal flux density in the air gap of the machine. Unlike the induction motors, they have smaller sizes, compact mechanical package and more importantly, they are more efficient than the induction motors. In addition, they can be used at the full torque at low speeds. Some of the drawbacks of the synchronous permanent magnet motors are higher initial price as this type of the motor is not the self-starting motor *ie* they require a variable frequency drive to operate. Additionally, in high precision applications or at low speeds, they might have some torque ripple known as the cogging torque that can deteriorate the motor performance. The cogging torque is generated when the sides of the rotor teeth line up with the stator teeth of the motor so that the stator and rotor teeth are aligned in the position of the lowest magnetic resistance. There are numerous methods to reduce the cogging torque. Almost all of them are related to the alterations of the motor design such as magnet pole shaping, magnet skewing, proper thickness of stator tips, smaller slot opening, increasing the number of slots/pole, additions of dummy slots or adding the magnet slot wages on stator slots [1,2].

In practice, the optimization of the stator slot opening is one of the most commonly used methods for reduction of the cogging torque which can include proper design of the stator slot opening or even completely closing the slots with magnet wages as too narrow slot opening can cause difficulties in mounting the stator winding [3–5]. The reduction of the cogging toque is especially important in direct-drive propulsion systems where there is no gear to minimize or absorb the cogging torque. Its minimization can be achieved through stator teeth pairing, optimal magnet pole-arc and stepped rotor skewing [6]. The proper design of the magnets plays a significant role in a good motor design in terms of the cogging torque minimization. The magnet segmentation, the magnet shifting, the magnet shaping, and the asymmetrical arrangements of magnets are some of the methods that have been analyzed for the minimization of the cogging torque [7–13]. Finding the optimal value of the magnet pole pitch or even using the hybrid permanent magnet excitation system composed of two different types of the magnet materials can lower the cogging torque [14, 15]. Finding the right parameters for the optimization is the first step in each optimization problem, in this case the minimization of the cogging torque. The second step is to choose the optimization method, which gives the global optimum within the family of possible solutions. The bifurcated teeth diameter and the pole angle have been optimized by using the hybrid optimization strategy composed of response surface methodology and the genetic algorithms (GA) for reducing the cogging torque of the synchronous permanent magnet motor [16]. Although time consuming, the GA has gained the popularity as a reliable

* Faculty of Electrical Engineering, University Goce Delcev, PO Box 201, 2000 Stip, North Macedonia, vasilija.sarac@ugd.edu.mk

DOI: 10.2478/jee-2019–0030, Print (till 2015) ISSN 1335-3632, On-line ISSN 1339-309X

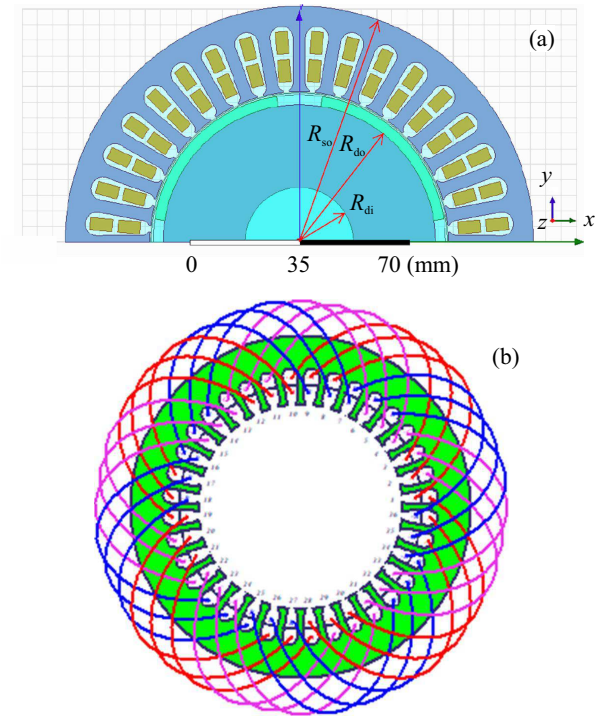

Fig. 1. Basic motor model-BM: (a) – cross-section, (b) – stator winding

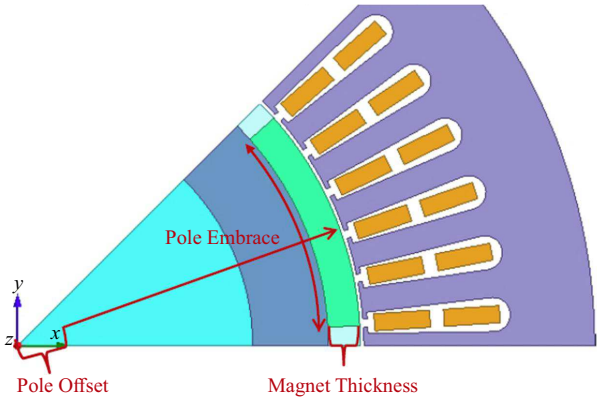

Fig. 2. Geometry of analyzed parameters [25]

method in finding the global optimum within the numerous possible solutions. In the authors previous work on the field of the cogging torque minimization, parameters were varied in the discrete steps within certain boundaries, using the parametric analysis, thus final solution resulted in the minimization of the cogging torque but without finding the global optimum or the best possible solution of the optimization problem [17]. Therefore, in this paper the GA method is applied in the minimization of the cogging torque by optimizing the three motor parameters: the magnet thickness, the magnet shape and the pole embrace *ie* the coverage of the rotor with the magnets or the magnet span. Firstly, a motor model suitable for computer-aided design is modeled and its accuracy is verified by comparing the output results of this model with the available data from the motor producer. Afterwards, the GA method is applied on the existing computer model, which yielded to the best set of data for the magnet thickness; the pole shape and the pole embrace that produce the minimal cogging torque. The GA had searched the complete space of the possible solutions and had found the best combination of these three parameters that yielded to the global minimum of the optimization function in this case the cogging torque. The results from the GA optimization regarding these three parameters were applied in the optimized model and the remaining operating characteristics were obtained. All the other remaining motor characteristics such as the current, the efficiency factor, the torque, the power factor and the magnet weight had been calculated for the both motor models - the basic (BM) and the optimized (OM). The comparison of the parameters and the characteristics of the two models give an insight into the impact that these three optimization parameters have on the cogging torque reduction but also on the overall motor operation. The accuracy of the motor design in terms of the magnetic flux density distribution and the core saturation is verified by the finite element analysis (FEA) as this numerical method has been proved to be a reliable tool in the machine design [18–23]. The FE models of the motors (BM and OM) had been derived and the magnetic flux density distribution in the air gap as well as in the motor cross-section was calculated as well. The both models, basic and optimized, have been compared; advantages and limitation of each of the models are discussed.

2 GA optimization and results

The basic computer model of synchronous permanent magnet motor is derived from asynchronous squirrel cage motor type 5AZ 100LA-4, product of company Rade Koncar [24], by replacing the squirrel cage winding with surface mounted magnets on the rotor. A more detailed study of the derivation of the synchronous permanent magnet motor with surface mounted magnets from asynchronous squirrel cage motor is given in authors previous work [17], where is also presented comparison of motor parameters and operating characteristics of both motors, taking into account that parameters and characteristics of asynchronous motor are obtained from the motor producer [24]. This derived model of the synchronous motor in [17] is designated here as basic motor model. It is modeled in Ansys Maxwell software that allows two types of motor models to be created, analytical model as well as the numerical model of the analyzed machine [25]. Both machine models require the exact motor geometry and the properties of all the materials to be entered in the computer model along with the adequate modeling of the stator winding and the magnet poles. Fig. 1 presents the cross-section of this model and the stator winding. Main motor dimension and winding parameters are presented in Tab. 1. Dimensions related to magnet poles are presented in Fig. 2.

Table 1. Main motor dimensions and winding parameters

Stator outer radius R_{so} (mm)	76
Rotor outer radius R_{do} (mm)	46.6
Rotor inner radius R_{di} (mm)	17
Motor length (mm)	100
Number of stator slots	36
Winding layers	2
Number of parallel branches	2
Conductors per slot	97
Coil pitch	7

Table 2. Comparison of BM and producer data

	BM	Producer data
Rated power (kW)	2.2	2.2
Rated current (A)	5.05	4.9
Rated torque (Nm)	14	14.9
Speed (rpm)	1500	1500

Table 3. Ranges of variation of optimization variables

Variable	Range	BM
Magnet thickness h_m (mm)	3 – 4	3.4
Pole offset α_p (mm)	0 – 10	0
Pole embrace b_p (-)	0.7 – 0.9	0.8

As an output from the BM the relevant data and the characteristics for the motor operation are obtained. The verification of the accuracy of the BM is done by comparing the obtained output results with the available data from the motor producer [24], relevant for comparison of these two types of these motors, new derived model of the synchronous motor, here designated as BM, and asynchronous squirrel cage motor. Table 2 presents this comparison.

The objective function of the optimization is the cogging torque, which should be minimized. The optimization is done by changing the magnet design *ie* the magnet thickness, the pole offset (the shape of the magnets) and the pole embrace (coverage of the rotor with the magnets). Figure 2 presents the optimization variables, where pole embrace represents the ratio of the pole arc to the pole pitch, pole offset is pole arc center offset from the rotor center while magnet thickness is the thickness of the magnets mounted on the rotor surface.

The ranges of variation of the optimization variables are presented in Tab. 3, which presents also the values of the optimziation variables which are used in the BM, only here they are fixed values as BM is actually the starting motor model that should be optimized.

The optimization model of the motor was created using GA method with random search. The created GA model has maximum number of generations 20, as parents has 20 individuals, as mating pool 20 individuals, as children 20 individuals and also in the next generation the number of the individuals is 20. Setting of the model was based on the recommendation from the software producer, and the time required the optimization problem to be solved. Cost function is optimized with respect to three calculation setups: cogging torque, average value of magnetic flux density in the air gap and magnet area. The first calculation setup for the cogging torque is defined by taking into consideration that the maximum cogging torque of 0.502 Nm is obtained from the motor model with pole embrace 0.7 mm, magnet thickness 3 mm and pole offset zero. Subjectively is chosen cogging torque to be reduced for more than ten times. The normalize solution range is 1 to 10. The second calculation setup defines the ranges of average value of magnetic flux density in the air gap B_{avg} obtained from the border values of the optimization variables *ie* it is adopted that Bavg should be within the interval 0.4 – 0.61 T. This also defines the second constrain which optimization process should satisfy. The third calculation setup defines the magnet area i.e. its range, found from the geometrical dimension of the magnet poles. Therefore, as a third constrain in the optimization process is imposed magnet area to be within 151 mm^2 to 258 mm^2, both numbers are found from the border values of optimization parameters. A more detailed explanation of setting the optimization model can be found in [25]. After the optimization is done, the results are available in a graphic form thus the variation of the cost function through the iterations is presented in Fig. 3. As the objective function is the cogging torque, which should be minimized, consequently the cost function should be minimized i.e. the set of the optimized variables for which the cost function is minimal represents the best solution of the optimization problem. Some of the optimization results, including the best set of the optimization variables for minimizing the cogging torque, are presented in Tab. 4.

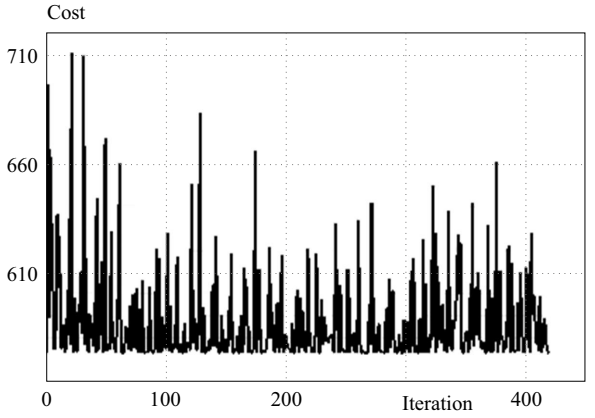

Fig. 3. Variation of the cost function

Table 4. Variation of cost function through iterations

Iteration no	Magnet thickness h_m (mm)	Pole embrace b_p (-)	Pole offset- α_{p} (mm)	Cost
82	3.405	0.7937	9.488	572.82
66	3.364	0.7964	9.189	572.83
229	3.396	0.7961	9.556	572.83
367	3.287	0.8044	8.129	572.84
164	3.342	0.752	8.332	572.85
192	3.418	0.7538	8.772	572.85
205	3.41	0.754	8.812	572.85
251	3.404	0.7636	9.34	572.85
310	3.422	0.7944	9.577	572.85
314	3.415	0.7959	9.51	572.85
162	3.366	0.7967	9.398	572.86
222	3.366	0.7983	9.388	572.86
224	3.443	0.794	9.693	572.86
260	3.377	0.7511	8.322	572.86
304	3.384	0.7843	9.43	572.86
316	3.455	0.7574	9.383	572.86
399	3.417	0.7939	9.832	572.86
404	3.298	0.7939	8.557	572.86
173	3.411	0.7611	9.355	572.87
267	3.357	0.7506	8.465	572.87
282	3.387	0.7961	9.692	572.87
319	3.358	0.7959	8.76	572.87
65	3.429	0.7499	9.119	572.88
115	3.377	0.7582	8.999	572.88

Table 5. Comparison of characteristics of BM and OM

Parameter	BM	OM
Rated power (kW)	2.2	2.2
Rated torque (Nm)	14.013	14.013
Rated current (A)	5.05	5.014
Rated speed (rpm)	1500	1500
Cogging torque (Nm)	0.3687	0.0169
Efficiency factor (%)	93.07	93.182
Air gap flux density (T)	0.489	0.581
Magnet weight (kg)	0.651	0.502
Core losses (W)	14.49	13.855
Copper losses (W)	149.398	147.199
Total losses (W)	163.89	161.054
No load current (A)	3.6944	3.544

In Tab. 4, the results are presented sorted per value of the cost function; the minimal cost function is on the top of the table. Figure 4 presents the two different rotor configurations of the basic (BM) and the optimized motor (OM) after the optimized variables h_{m}, b_{p} and α_{p} had been implemented in the design of the optimized model. Here it must be noted the rotor configuration in Fig. 4(b) is automatically obtained from motor computer model in Maxwell software when obtained parameters from the optimization, $h_{\mathrm{m}} = 3.405$ mm, $b_{\mathrm{p}} = 0.79$ and $\alpha_{\mathrm{p}} = 9.49$ mm, are input into the computer model of the motor. Drawing the motor configuration with automated software for professional design of electrical machines allows minimization of drawing errors, often present when machines are drawn in the graphic softwares, thus directly linking the motor geometry with the software module for analytical calculations of the machine parameters and output characteristics [25].

With the obtained set of the optimized variables $h_{\mathrm{m}} = 3.405$ mm, $b_{\mathrm{p}} = 0.79$ and $\alpha_{\mathrm{p}} = 9.49$ mm, the new optimized model of the motor (OM) had been recalculated not only for the value of the cogging torque but also for the other operating characteristics presented in Tab. 5. So the output characteristics of the OM in Tab. 5 are obtained when in the BM are replaced the best set of optimized variables *ie* $h_{\mathrm{m}} = 3.405$ mm, $b_{\mathrm{p}} = 0.79$ and $\alpha_{\mathrm{p}} = 9.49$ mm instead of $h_{\mathrm{m}} = 3.4$ mm, $b_{\mathrm{p}} = 0.8$ and $\alpha_{\mathrm{p}} = 0$ mm. The created computer model for analytical calculation of the motor allows obtaining the output characteristics of the optimized motor such as power, current, efficiency, speed *etc* , when all motor design parameters

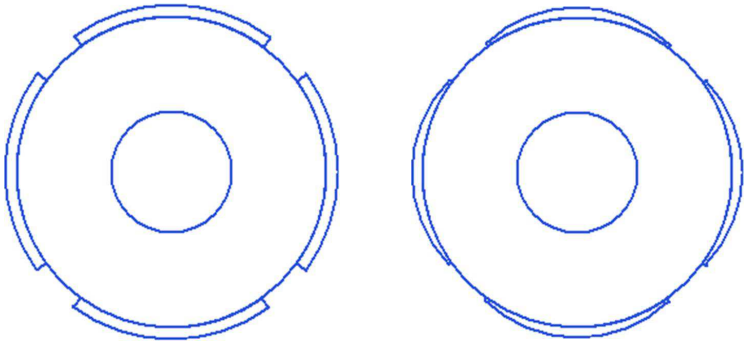

Fig. 4. Rotor configuration: (a) – BM, (b) – OM

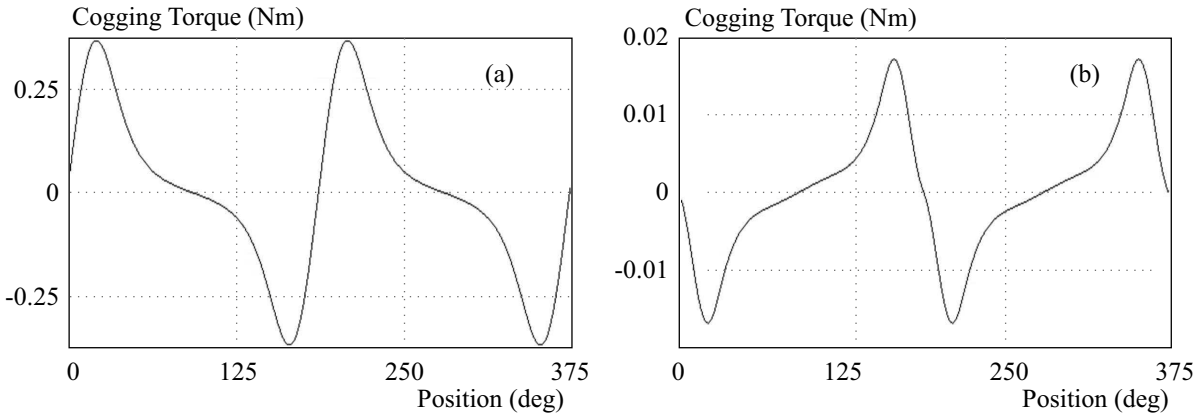

Fig. 5. Cogging torque as function of the air-gap position: (a) – BM, (b) – OM

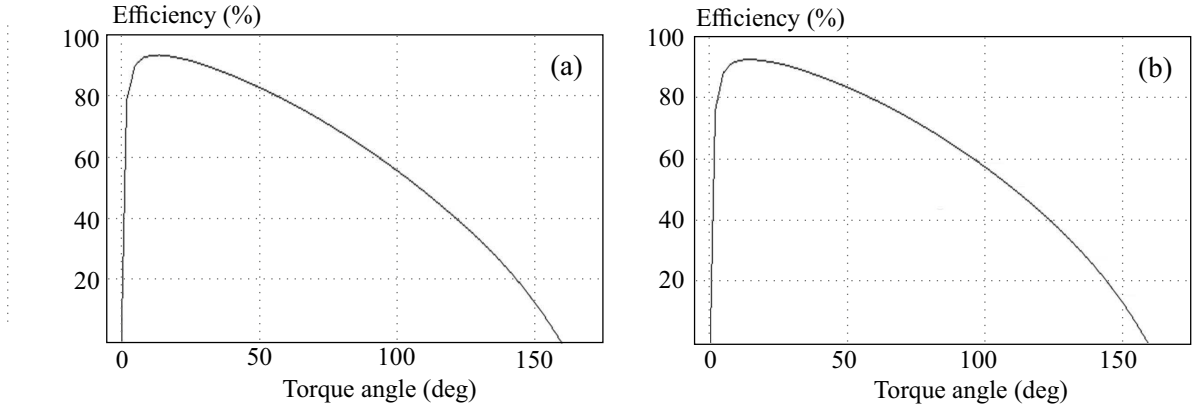

Fig. 6. Efficiency as a function of Torque angle: (a) – BM, (b) – OM

are clearly defined. Table 5 also presents the operating characteristics of the basic model, in which h_{m} is 3.4 mm, b_{p} is 0.8 and α_{p} is 0 mm, thus allowing direct comparison of the both motor models-the basic (BM) and the optimized (OM).

As an output from the analytical model of BM and OM the output characteristics of both motor models are obtained in graphical form. The presented characteristics are result of the calculation of the motor models (BM and OM) in Maxwell software, specialized for the design of electrical machines, and they are automatically generated when the calculation of the machine is finished. The software uses the quadrature representation of the machine per d and q axis of symmetry and general presentation of common analytical expressions can be found in [25]. Figure 5 presents the cogging torque while Fig. 6 presents the efficiency factor. Figure 7 presents the air gap flux density, based on the analytical calculations of the motor models. The air gap flux density under the influence of stator slots can be found from [27]

$$B_{\mathrm{gs}}(\theta) = K_{\mathrm{sl}}(\theta) B_{\mathrm{g}}(\theta) \tag{1}$$

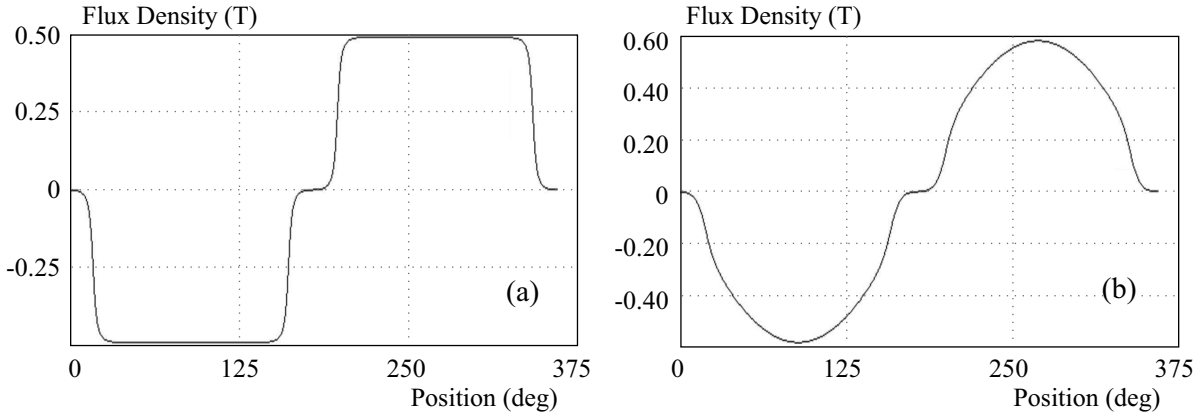

Fig. 7. Air gap flux density as a function of the air-gap position: (a) – BM, (b) – OM

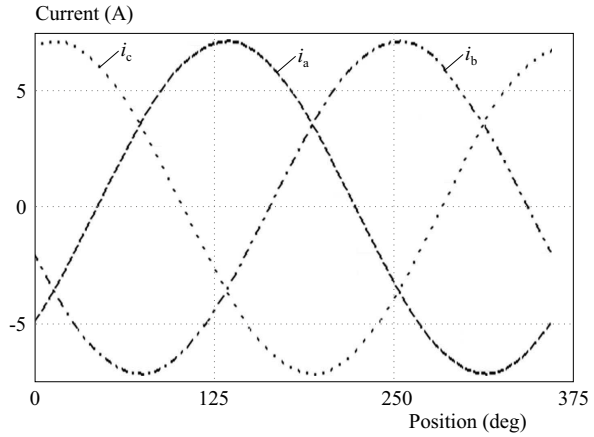

Fig. 8. Winding currents as a function of the air-gap position at optimized model

where

$$B_{\mathrm{g}}(\theta) = B_{\mathrm{ar}}(R_{\mathrm{s}}, \theta) \tag{2}$$

Equation (2) is fixed to the rotor coordinate system. R_{s} is the radius to stator air gap interface

$$B_{\mathrm{ar}}(R_{\mathrm{s}}, \theta) = \sum_{-\infty}^{\infty} B_{\mathrm{arn}} e^{jn\theta} \tag{3}$$

B_{arn} are the Fourier series coefficients and θ is the angular position in electrical degrees. Above, K_{sl} is the slot correction factor

$$K_{\mathrm{sl}} = \frac{1 + \dfrac{h_m}{g\mu_R}}{\dfrac{g(\theta)}{g} + \dfrac{h_m}{g\mu_R}} \tag{4}$$

where h_m is the magnet thickness along the direction of magnetization and μ_R is the relative recoil permeability. The term $g(\theta)/g$ is the normalized air gap length, where g is the air gap length and $g(\theta)$ describes the air gap variation as one moves from tooth to slot to tooth on the stator [27].

The currents in the stator winding in the optimized model are presented in Fig. 8. From the Tab. 5 it can be noticed that rated current in basic and optimized model is almost identical as in the BM it is 5.05 A and in the optimized model is 5.014 A. Therefore, Fig. 8 presents the diagrams of the motor currents in all three phases only for the optimized model. Simultaneously, it confirms the presented result of motor current in Tab. 5 as the obtained maximum of the current in Fig.8 is 7 A or RMS value of 4.96 A. The similar conclusions can be drawn by comparing the presented results of cogging toque, efficiency factor and air gap flux density in Tab. 5 and in Fig. 5 to Fig. 7.

3 FE models and results

The optimization of the cogging torque with the GA and the analytical calculations of the motor parameters and the characteristics allow estimation of the motor design and its behavior at various operating modes. As the analytical calculation of the motor design uses assumed and approximated values of the magnetic flux density in the air gap as well as in the various parts of the motor construction, FE is often used for more accurate calculation of the magnetic flux density in the motor cross-section. The FE models allow accurate estimation of the magnetic core saturation thus they a necessary part of each the motor analysis in terms of the verification the motor design. The two FE models for the basic and the optimized motor were derived. Consequently, the magnetic flux density distribution in the motor cross-section is presented in Fig. 9.

From the presented results in Fig. 9, it can be observed that the optimized model has the lower flux density than the basic model. The both models in some parts of the stator yoke have the high flux density near to the point of the core saturation, which, could be improved, with some alteration in motor design. *ie* greater magnet thickness that can reduce the current in the main stator winding and consequently the magnetic flux density in stator yoke. Figure 10 presents the distribution of the air gap flux density in the both motor models, calculated by FEA.

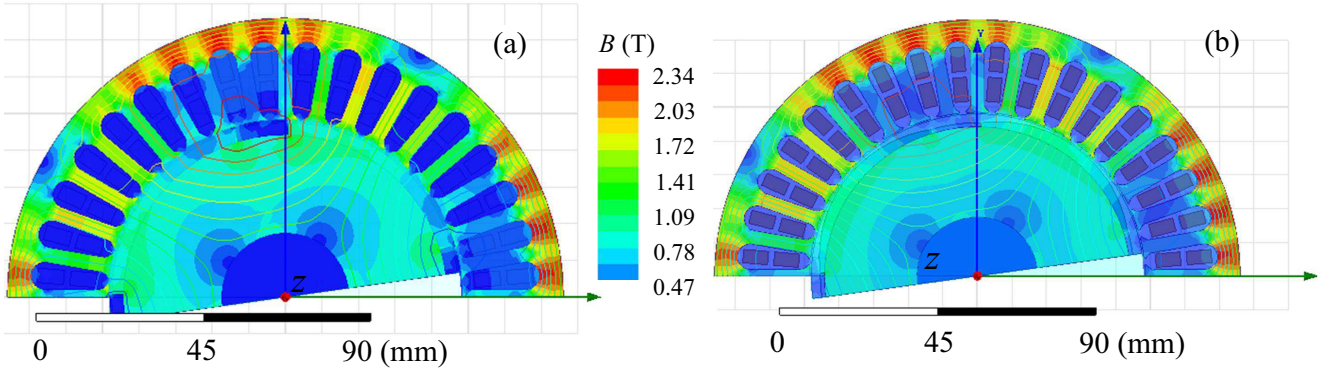

Fig. 9. Flux density distribution in motor air gap:(a) – BM, (b) - OM

Figure 11 presents the motor torque of both models calculated for the rated load and the constant synchronous speed from FEA.

From the results in Fig. 11, it can be observed that transients in torque curve are not so emphasized in case of the optimized model where the cogging torque is minimized. In addition, the average values of the torque are calculated for the last time interval of twenty milliseconds for the both models.

4 Discussion

The analyzed synchronous motor is aimed for the constant power operation. Therefore, in both motor models – BM and OM the output power remains constant as well as the output torque. The current in stator winding was insignificantly reduced due to the increased air gap flux density. The flux density in air gap was not only increased due to the alterations in magnet design, but also the distribution of the flux density became more sinusoidal. A sinusoidal distribution of the air gap flux density contributes to the smoother torque. There are several methods related to obtaining the sinusoidal distribution of the flux density in the air gap. Some of them are magnetization of the permanent magnets oriented along the rotor radius or in parallel to the pole axis or modulated poles with different permanent magnet materials as an alternative to the complex magnetization systems [26]. The pole shaping as it was done in this optimization procedure can also contribute to the sinusoidal flux density distribution in the air gap. From Tab. 5 it can be observed that the reduced current in the stator winding resulted in the reduced copper losses. The core losses were also reduced due to the reduced weight and the consumption of the permanent magnet material. Due to the reduced total losses in the optimized model, the efficiency factor was also improved from 93.07 % to 93.182 %. The cogging torque was significantly reduced from 0.368 Nm to 0.0169 Nm. The reduction of the cogging torque was achieved without changing the motor output power or operating torque therefore, the motor characteristics were not deteriorated. As it can be observed from the results of the optimization variables, the most significant parameter in the reduction of the cogging torque for the analyzed motor is the pole shape. The other two parameters, magnet thickness and pole embrace, although were varied in relatively wide ranges, their change in the optimized model was insignificant. In the authors previous work, the magnet thickness was checked against the demagnetization as too thin magnets can be easily demagnetized due to the reaction of the magnetic field from the stator winding to the field from the permanent magnets [17]. As in this case the magnet thickness remains almost unchanged after the optimization, there is no need to repeat the calculation for the magnet demagnetization.

The magnet shaping, although effective as a measure of reducing the cogging torque, encounters several technical problems in manufacturing. Rare earth magnets are machined by grinding which may considerably affect the magnet cost. Therefore from the economic point of view maintain simple geometries and wide tolerance is desirable. Sintering is also one of the methods used for manufacturing rare earth magnets. It is done by compacting the fine powders at high pressure in aligning magnetic field, than sintering to fuse into a solid shape. The intricacy of shapes that can be thus pressed is limited [28]. Pressure bonding or injection molding the powders in a carrier matrix can also be used in manufacturing the rare earth magnets and the ferrite magnets. In this case, the density of magnet material is lower, yielding the lower magnetic properties. However, the bonded or injection molded magnets may be fabricated in relatively intricate shapes. Finally, ferrite magnets are made by extruding magnet powder in a flexible carrier matrix. Magnet powder densities and therefore magnetic properties are even lower than the bonded or injection molded form. The advantage is that they can be easily cut or punched to shape [28].

It can be concluded that the basic motor was properly dimensioned regarding the magnet thickness and span in terms of minimizing the cogging torque. The both models have the high flux density in the stator yoke, close to the point of the magnetic core saturation. The core saturation can be avoided by reducing the stator current. Consequently, the magnetic field from the magnets should be

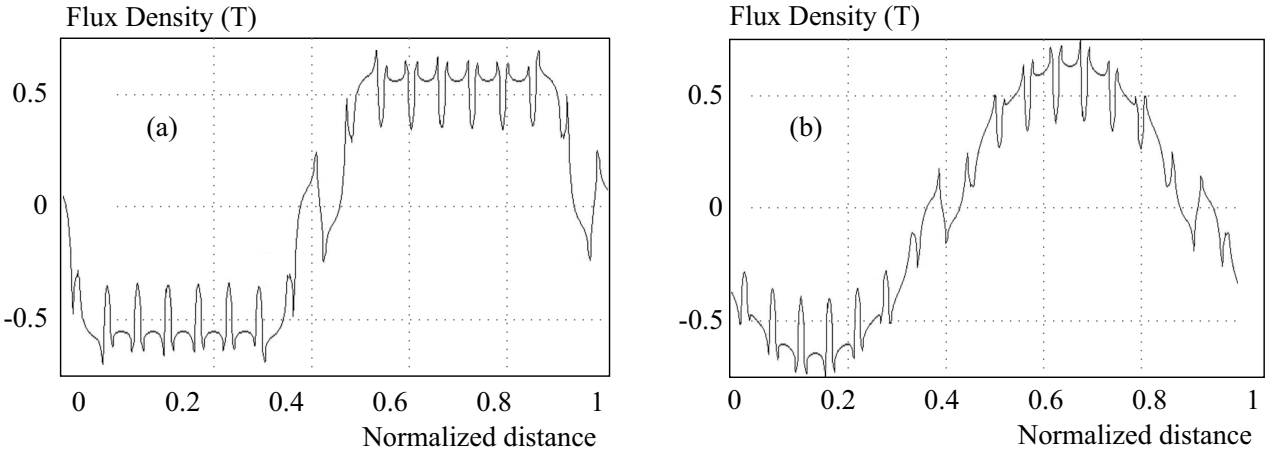

Fig. 10. Flux density distribution in motor air gap: (a) – BM, (b) – OM

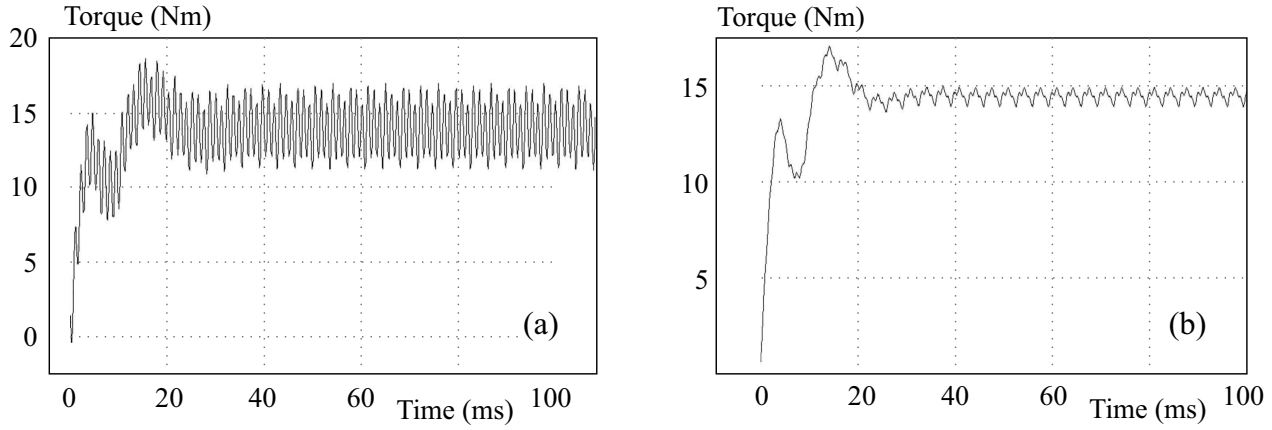

Fig. 11. Motor torque: (a) – BM with average torque 14 Nm, (b) – OM with average torque 14.45 Nm

increased *ie* the magnet thickness should be increased in order to maintain unchanged the air gap flux density and the torque. However, this will contribute to the change of the cogging torque *ie* it will not be minimized anymore. The increase of magnet thickness will certainly increase the magnet weight; therefore, the cost of the motor itself will be also increased. The reduction of the cogging torque contributed to the smoother motor torque as can be observed from Fig. 11. The obtained values of the torque in FE models, after the transients are suppressed, are close to the torque value in the analytical models and the producer data, thus confirming the accuracy of the derived models – the analytical and the numerical.

5 Conclusion

In this paper, the method of genetic algorithms is applied in the optimization i.e. the minimization of the cogging torque in the synchronous permanent magnet motor with surface mounted magnets. Three optimization variables were included in the optimization problem. All the three variables are related to the design of the rotor poles *ie* the magnet thickness, the magnet shape and the magnet span. Although time consuming, the GA allows finding the global optimum from the wide area of the possible solutions *ie* finding of the best combination of all the three parameters that, minimize the cogging torque. Due to the optimization of these three variables, significant reduction of the cogging torque is achieved from 0.368 Nm to 0.0169 Nm. As the other operating characteristics of the motor are also important, they are calculated from the analytical model of the basic and optimized motor. From the obtained results, it can be observed that besides minimizing the cogging torque and smoother motor torque, the operating torque of the motor remains unchanged as well as the output power. This is certainly beneficial for the optimized model, as no other operating characteristics are deteriorated. In the optimized model, the total losses are decreased, and the efficiency factor is improved. Further, due to the magnet shaping, the magnet weight is reduced and consequently the motor weight. As the cost of the permanent magnets is a considerable portion of the overall motor costs this can lead to the more cost-efficient design of the motor. On the other hand, the magnet shaping adds additional costs to the magnet production, so a more detailed techno-economical analysis is needed for estimating all the benefits and the drawbacks of the optimized model. The both models are operating near to the

point of the saturation of the motor core, so in the further research some alterations of the motor design should be considered. Yet, each improvement of the design is a trade-off between the operating characteristics, the dimensions and the costs of the machine.

References

[1] T. Srisiriwanna and M. Konghirun, "A Study of Cogging Torque Reduction Methods in Brushless DC Motor", *ECTI Transactions on Electrical Engineering Electronics Communications* vol. 10, no. 2.

[2] Z. Q. Zhu, and D. Howe, "Influence of Design Parameters on Cogging Torque in Permanent Magnet Machines", *IEEE Transactions on energy Conversion* vol. 15, no. 4, pp. 407–412, December 2000.

[3] L. Zhu, S. Z. Jiang, Z. Q. Zhu, and C. C. Chan, "Optimal Slot Opening in Permanent Magnet Machines for Minimum Cogging Torque", *Prezglad Elektrotechniczny* vol. 87, no. 3, pp. 315–319, 2011.

[4] N. Levin, S. Orlova, V. Pugachov, B. Ose-Zala, and E. Jakobson, "Methods to Reduce the Cogging Torque in Permanent Magnet Synchronous Machines", *Elektronika ir Elektrotechnika* vol. 19, no. 1, pp. 24–15, 2013.

[5] T. Tudorache and M. Modreanu, "Design Solutions for Reducing the Cogging Torque of PMSM", *Advances in Electrical Computer Engineering* vol. 13, no. 3, pp. 59–64, 2013.

[6] W. Fei and P. C. K. Luk, "A New Technique of Cogging Torque Suppression in Direct-Drive Permanent Magnet Brushless Machines", *IEEE Transactions on Industry Application* vol. 46, no. 4, pp. 1332–1340, 2010.

[7] A. Ghassemi, "Cogging Torque Reduction Optimization in Surface-Mounted Permanent Magnet Motor using Magnet Segmentation Method", *Electric Power Components Systems* vol. 42, no. 12, pp. 1239–1248, 2014.

[8] L. Dosiek and P. Pillay, "Cogging Torque Reduction in Permanent Magnet Machines", *IEEE Transactions on Industry Applications* vol. 43, no. 6, pp. 1565–1571, 2007.

[9] D. A. Gonzalez, J. A. Tapia, and A. L. Bettancourt, "Design Consideration to Reduce Cogging Torque in Axial Flux Permanent-Magnet Machines", *IEEE Transactions on Magnetics* vol. 43, no. 8, pp. 3435–3440, 2007.

[10] Y. Özoğlu, "New Magnet Shape for Reducing Torque Ripple in an Outer-Rotor Permanent-Magnet Machine", *Turkish Journal of Electrical Engineering & Computer Sciences* vol. 25, pp. 4381–4397, 2017.

[11] Chun-Yu Hsiao Sheng-Nian Yeh and Jonq-Chin Hwang, "A Novel Cogging Torque Simulation Method for Permanent-Magnet Synchronous Machines", *Energies* vol. 4, no. 12, pp. 2166–2179, 2011.

[12] I. Trifu, "Research on Reducing Cogging Torque in Permanent Magnet Synchronous Generators", *Scientific bulletin, Series C, Electrical Engineering and Computer Science* vol. 77, no. 3, pp. 225–234, 2015.

[13] J. W. Jiang, B. Bilgin, Y. Yang, A. Sathyan, H. Dadkhah, and A. Emadi, "Rotor Skew Pattern Design Optimization for Cogging Torque Reduction", *IET Electrical Systems in Transportation* vol. 6, no. 2, pp. 126–135, 2016.

[14] S. Jagasics and I. Vajda, "Cogging Torque Reduction by Magnet Pole Pairing Technique", *Acta Polytechnica Hungarica* vol. 13, no. 4, pp. 107–130, 2016.

[15] L. Knypiński, L. Nowak, and A. Demenko, "Optimization of Synchronous Motor with Hybrid Permanent Magnet Excitation System", *The International Journal for Computation Mathematics in Electrical and Electronic Engineering*, vol. 34, no. 2, pp. 448–455, 2015.

[16] J. Min-Jae Kim, J. Lim, Jang-Ho Seo and Hyun-Kyo Jung, " Hybrid Oprimization Strategy using Response Surface Methodology Genetic Algorithm for Reducing Cogging Torque of SPM", *Journal of Electrical Engineering & Technology* vol. 6, no. 2, pp. 202–207, 2011.

[17] V. Sarac and D. Iliev, "Synchronous Motor of Permanent Magnet Compared to Asynchronous Induction Motor, *Electrotehnica, Electronica, Aitomatica* vol. 65, no. 4, pp. 51–58, 2017.

[18] R. Trifa, C. Martis, K. Biro, and A. M. Gazdac, "Design Analysis of Permanent Magnet Synchronous Machine for Automotive Electromechanical Braking System", *Prezglad Electrotechniczny* vol. 88, no. 7b, pp. 141–144, 2012.

[19] G. M. Kiss and I. Vajda, "Co-Simulation of an Inverter Fed Permanent Magnet Synchronous Machine", *Electrical, Control Communication Engineering* vol. 6, no. 1, pp. 19–25, 2014.

[20] R. Tanabe and K. Akatsu, "Advanced Torque Control of Permanent Magnet Synchronous Motor using Finite Element Analysis Based Motor Model with a Real-Time Simulator", *IEEJ Journal of Industry Applications* vol. 6, no. 3, pp. 173–180.

[21] E. Öksüztepe, Z. Omac, M. Polat, H. Çelik, A. Selçuk, and H. Kürüm, "Senseless Field Oriented Control of Nonsinusoidal Flux-Distribution Permanent Magnet Synchronous Motor with FEM Based ANN Observer", *Turkish Journal of Electrical Engineering & Computer Science* vol. 24, pp. 2994–3010, 2016.

[22] E. M. Barhoumi, A. G. Abo-Khalil, Y. Berrouche, and F. Wurtz, "Analysis Comparison of end Effects in Linear Switched Reluctance Hybrid Motors", *Journal of Electrical Engineering* vol. 68, no. 2, pp. 138–142, 2017.

[23] E. El-kharashi and H. M. Hassanien, "Reconstruction of the Switched Reluctance Motor Stator", *Journal of Electrical Engineering* vol. 63, no. 1, pp. 3–12, 2012.

[24] Končar-MES d.d., Ansys Inc., "Three phase squirrel cage induction motors, catalogue.

[25] Ansys Inc., "Maxwell 2D-users guide", 2010.

[26] S. Vaez-Zadeh, "Control of Permanent Magnet Synchronous Motor", *Oxford University Press*, pp. 22–23, 2018.

[27] D. Hanselmasn, "Brushless Permanent Magnet Motor Design", *Magna Physics Publishing*, Second Edition, pp. 155–156, 2006.

[28] "Magnetics101-Design Guide, Integrated magnets" https://www.intemag.com /magnet-design-guide [accessed 22.05.2019].

Received 13 February 2019

Vasilija Sarac associate professor of the Faculty of Electrical Engineering at University Goce Delcev, Stip, Republic of North Macedonia. Her main research interests include design, simulation and optimization methods of electrical machines and power converters